

1                   **Major changes in plastid protein import and the origin of the Chloroplastida**

2

3                   <sup>1</sup>Michael Knopp\*, <sup>1</sup>Sriram G. Garg\*, <sup>1</sup>Maria Handrich, <sup>1</sup>Sven B. Gould<sup>#</sup>

4

5                   <sup>1</sup>Institute for Molecular Evolution, HH-University Düsseldorf, 40225 Düsseldorf, Germany

6

7                   \*These authors contributed equally

8                   <sup>#</sup>Corresponding author: [gould@hhu.de](mailto:gould@hhu.de)

9

10                  **Abstract**

11                  While core components of plastid protein import (Toc and Tic) and the principle of using N-  
12                  terminal targeting sequences (NTS) are conserved, lineage-specific differences are known.  
13                  Rhodophytes and glaucophytes carry a conserved NTS motif, which was lost in the green  
14                  lineage that also added novel proteins to Toc and Tic. Here we compare the components of  
15                  plastid protein import and generated RNA-Seq, pigment profile and trans-electron microscopy  
16                  data based on high-light stress from representatives of the three archaeplastidal groups. In light  
17                  of plastid protein targeting, we compare the response to high-light stress of archaeplastidal  
18                  representatives based on RNA-Seq, pigment profile and trans-electron microscopy data. Like  
19                  land plants, the chlorophyte *Chlamydomonas reinhardtii* displays a broad respond to high-light  
20                  stress, not observed to the same degree in the glaucophyte *Cyanophora paradoxa* or the  
21                  rhodophyte *Porphyridium purpureum*. We find that only the green lineage encodes a conserved  
22                  duplicate of the outer plastid membrane protein channel Oep80, namely Toc75 and suggest that  
23                  the ability to respond to high-light stress entailed evolutionary changes in protein import,  
24                  including the departure from phenylalanine-based targeting and the introduction of a green-  
25                  specific Toc75 next to other import components unique to Chloroplastida. One consequence of  
26                  relaxed NTS specificity was the origin of dual-targeting of plastid derived proteins to  
27                  mitochondria and vice versa, using a single ambiguous NTS. Changes in the plastid protein  
28                  import enabled the green lineage to import proteins at a more efficient rate, including those  
29                  required for high-light stress response, a prerequisite for the colonization of land.

30

31                  **Keyword:** Chloroplast evolution, protein import, Toc75, protein targeting, dual-targeting

32 **High-lights**

33 - Loss of Phe-based N-terminal targeting sequences (NTS) triggered the origin of dual-  
34 targeting using a single ambiguous NTS  
35 - The Chloroplastida evolved a green-specific Toc75 for high throughput import, next to a  
36 universal and ancient Omp85 present in all Archaeplastida  
37 - A broad response to high-light stress appears unique to Chloroplastida  
38 - Relaxation of functional constraints allowed a broader modification of the green Toc/Tic  
39 machinery  
40 - Critical changes in plastid targeting enabled the origin and success of the Chloroplastida  
41 and their later conquer of land

42

43 **Introduction**

44 Mitochondria and plastids are of endosymbiotic origin and compartments surrounded by a  
45 double-membrane<sup>1,2</sup>. Most possess their own genomes, but the bulk of their former coding  
46 capacity was either lost or integrated into the nuclear genome<sup>3,4</sup>. As a consequence, most of  
47 their proteins are post-translationally imported. Guiding of precursor proteins to the matrix or  
48 stroma typically relies on N-terminal targeting sequences (NTS)<sup>5-7</sup>, although some exceptions  
49 are known<sup>8-10</sup>. Archaeplastidal plastids have a monophyletic origin<sup>11-13</sup>, which is also evident  
50 by the conserved nature plastid import components, a reliable indicator for the monophyly of  
51 organelles<sup>14-16</sup>.

52 While sharing a single origin, the plastids of the three algal lineages have evolved considerable  
53 differences since their divergence more than a billion years ago<sup>17,18</sup>. These include, but are not  
54 limited to: (i) the thickness of a remaining peptidoglycan layer<sup>19,20</sup>, (ii) the localisation of starch  
55 deposits<sup>21</sup>, (iii) the coding capacity of their genomes<sup>3,22</sup>, (iv) pigment composition and the types  
56 of antenna complexes used<sup>23</sup>, (v) the absence or presence of a xanthophyll cycle<sup>24</sup> and (vi) the  
57 composition of the protein import machinery<sup>25,26</sup>. It raises the question to what degree the two  
58 – critical changes in protein import and changes in plastid biology – are connected, and whether  
59 one of the two conditioned or enabled the other. Though most information about plastid protein  
60 targeting stems from the green lineage<sup>27</sup>, several remarkable differences between the protein  
61 import in plastids of the three algal groups (Glauco phyta, Rhodophyta, and Chloroplastida) are  
62 known.

63 One important difference concerns the NTS that targets proteins to the plastid stroma.  
64 Rhodophytes and glauco phytes employ a single amino acid-based motif to target proteins to  
65 their plastids<sup>16,27-29</sup>. In most cases this amino acid is a phenylalanine, less frequently other bulky  
66 aromatic amino acids<sup>27,30</sup>. The F-based motif is found at the very N-terminus of the NTS (Fig.  
67 1) and even retained in organisms with secondary plastids of red algal origin, such as the  
68 cryptophyte *Guillardia theta*, the diatom *Phaeodactylum tricornutum* and the parasite  
69 *Toxoplasma gondii*<sup>31</sup>. It is uncertain why the F-based motif was lost in Chloroplastida, but it  
70 came with several changes such as a rise in phosphorylatable serine residues that might help in  
71 avoiding erroneous targeting to the mitochondria<sup>32,33</sup>.

72 Despite a tendency towards organelle specificity, eukaryotes also target many proteins  
73 simultaneously to two different compartments, a process known as dual-targeting. Dual-

74 targeting can affect different combinations of compartments<sup>34,35</sup>, in plants also mitochondria  
75 and plastids. About 100 proteins are dually targeted to the mitochondria and plastids of  
76 *Arabidopsis thaliana* after their translation<sup>35,36</sup>. This large number is a consequence of the  
77 similarity between the two import mechanisms performed by Tom/Tim (translocator of the  
78 outer and inner mitochondrial membrane) and Toc/Tic (translocator of the outer and inner  
79 chloroplast membrane)<sup>5,32</sup>. In *A. thaliana*, a duplicate of the Toc64 receptor localizes to the  
80 outer mitochondrial membrane and now functions in mitochondrial import<sup>37</sup>. Both *Arabidopsis*  
81 organelles also use the same targeting-associated PURPLE ACID PHOSPHATASE2 (*AtPAP2*)  
82 at their outer membranes<sup>38,39</sup>. The extent of dual-targeting in non-chloroplastidial species  
83 remains largely unexplored.

84 To investigate plastid targeting in a comparative approach across the three main algal lineages,  
85 we generated RNA-Seq, pigment profile, and trans-electron microscopy data from three  
86 different conditions (with high-light stress as the stimulus) for the chlorophyte  
87 *Chlamydomonas reinhardtii*, the rhodophyte *Porphyridium purpureum* and the glaucophyte  
88 *Cyanophora paradoxa*. The data were compared and evaluated in light of evolutionary changes  
89 regarding protein import. Our analysis connects the loss of F-based targeting and the emergence  
90 of new critical import proteins in the ancestor of the green lineage, with a series of critical  
91 changes.

92

### 93 **Material and Methods**

#### 94 *Culturing*

95 Algae were grown in their respective media (see SAG Göttingen or ncma.bigelow.org for  
96 recipes) in aerated flasks at 20°C and illuminated with 50µE under a 12/12h day-night cycle.  
97 RNA was isolated from cells growing in the exponential phase either at 6h into the day, 6h into  
98 the night or after 1h of high-light treatment at 600µE. RNA was isolated, sequenced and  
99 assembled exactly as described previously<sup>40</sup> and based on pooled biological triplicates and  
100 independently sequenced technical triplicates.

101

#### 102 *Rapid light curves and pigment profiles*

103 The relative electron transport rates (rETR) of the different algae were measured with use of  
104 the FluorCam FC 800MF (Photo Systems Instruments) with modulated red light (emission at  
105 625nm and bandwidth of 40nm) as a source of measuring light (<0.1µmol quanta m<sup>-2</sup> s<sup>-1</sup>) and  
106 modulated blue light as saturation pulse (> 8000µmol quanta m<sup>-2</sup> s<sup>-1</sup>) (Suppl. Fig. 1). The algae  
107 samples were dark adapted for 5 min and repeatedly submitted to increasing light intensities  
108 (13, 48, 122, 160, 200, 235, 305, 375, 542, 670 µmol quanta m<sup>-2</sup> s<sup>-1</sup>) every 11 min. The exported  
109 numeric values were fitted according to Eilers & Peeters, 1988. For each pigment extraction  
110 the pellet of 50 ml culture was resuspended with 100% acetone, homogenized and kept at -20°C  
111 over night. On the next day extracts were centrifuged and supernatant was filtered once through  
112 a 200 nm polytetrafluoroethylene membrane and then analyzed by reversed-phage high  
113 pressure liquid chromatography (HPLC) with ultraviolet/visible spectroscopy detection  
114 (Hitachi/Merck). Pigment concentrations were determined using external pigment standards  
115 isolated from spinach thylakoids<sup>56</sup>.

116

117 *Microscopy*

118 For trans-electron microscopy cells were centrifuged at 800 x g and pellet was washed twice  
119 with PBS. Afterwards pellets were carefully resuspended with 2,5 % glutaraldehyde in 0,1 M  
120 cacodylate buffer and incubated for 2-3 days at 4°C. Fixed cells were then centrifuged and  
121 pellets was washed four times with 0,1 M cacodylate buffer with a minimum of 10 min  
122 incubation time and centrifugation for 2 min at 13.000 rpm. For contrasting, samples were  
123 resuspended in 2% Osmium(VIII)-oxid + 0,8% potassium hexacyanoferrate and incubated for  
124 1 h at room temperature. Then cells were washed again five times and after addition of 3,5 %  
125 agarose and resuspension cells were incubated on ice for a minimum of 10 min until agarose  
126 became hardened. Tube tips were cut using a guillotine and the solid agar embedded pellet was  
127 pulled out and transferred to a small glass container (40 x 19 mm, 5 ml, with plastic lids).  
128 Dehydration of cell pellets was achieved using an ascending ethanol washing series starting  
129 with 60% ethanol (1 x 10 min), followed by 70% (overnight at 4°C), 80% (2 x 10 min), 90%  
130 (2 x 10 min) and 100% (1 x 10 min), finishing with 100% ethanol + molecular strainer (1 x 10  
131 min) and propylenoxid (1 x 15 min). Afterwards epoxide resin/propylenoxid mixtures were  
132 added to the samples with increasing epoxide resin concentrations. First, a 1h incubation with  
133 epoxide resin/propylenoxid (1:2) was followed by a 1h incubation with epoxid  
134 resin/propylenoxid (1:1) and finally an overnight incubation with epoxide resin/propylenoxid  
135 (2:1) was performed. Freshly prepared epoxide resin was added the next day and samples  
136 incubated for four hours in a vacuum to remove any remaining oxygen within the epoxide  
137 resin/cell pellet solution. Finally, pellets were cut in approx. 1 mm slices with a razor blade and  
138 placed onto the tip of a notch on a rubber mat and completely covered with epoxide resin. After  
139 that epoxide resin filled mats were incubated for 24 h at 40°C followed by 24 h incubation at  
140 60°C for complete polymerization. Probes were then cut using a ultramicroton, placed on  
141 monitoring grids and examined using trans-electron microscopy (Zeiss EM902). For the  
142 analysis of thylakoid stacks, the distances within 10 cells were counted using Fiji<sup>57</sup>. For each  
143 graph 10 cells were analyzed and within each cell 10 different areas counted.

144

145 *Identification of differentially expressed genes and annotation*

146 Subsequent to the assembly via Trinity<sup>41</sup> (r2013-02-25), edgeR<sup>42</sup> was used to calculate the  
147 number of differentially expressed genes. The criteria for the identification were a logarithmic  
148 fold change of at least 2 and significance of 0.001 or lower. Since this approach only detected  
149 91 differentially expressed genes for *P. purpureum*, the significance cutoff was lowered to 0.05  
150 as suggested by the EdgeR manual (<https://github.com/trinityrnaseq/trinityrnaseq/wiki>). The  
151 transcripts were ranked according to mean expression values for all three light conditions and  
152 each organism. Protein annotation was performed by a BLAST search of all CDS against 112  
153 Refseq plant and algae genomes. All BLAST hits with at least 25% local identity and a  
154 maximum E-value of  $1 \times 10^{-10}$  were used for annotation. In cases where the hit did not provide  
155 enough information (hypothetical proteins, predicted proteins) the next best non-hypothetical  
156 hit was selected.

157

158 *Phylogenomic analysis*

159 The sequence dataset for the phylogenetic analysis of the Toc75/Oep80 homologs consists of  
160 77 amino acid sequences from Chlorophytes, Rhodophytes, Cyanobacteria, Plants and one  
161 Glaucophyte. We consulted Inoue and Potter 2004 to obtain 39 amino acid sequences of Toc75  
162 and Oep80 homologs from either the Refseq<sup>43</sup> or GenBank<sup>44</sup> database via their respective gene  
163 identifiers (Suppl. table 1)<sup>45</sup>. Additionally, 28 genomes from Chlorophytes, Rhodophytes<sup>46</sup> and  
164 one Glaucophyte were downloaded either from the Refseq, GenBank or the JGI Genome  
165 Portal<sup>47</sup> (Suppl. table 1). The initial set of sequences was used as query sequences to search for  
166 Toc75 and Oep80 homologs via BLASTp (version 2.5.0)<sup>48,49</sup>. All non-redundant hits from each  
167 subject genome with at least 25% local identity and a maximum E-value of 0.001 were added  
168 to the sequence set. Blast hits of Oep80 and Toc75 sequences of the initial sequence set were  
169 named pOep80 and pToc75 respectively.

170 Multiple protein sequence alignments were constructed using MAFFT (version 7.299b) with  
171 the parameters “--maxiterate 1000” and “--localpair”<sup>50</sup>. The initial multiple protein sequence  
172 alignment was used to check the quality of identified homologs, resulting in the removal of  
173 sequences that differed drastically in overall amino acid composition. The multiple amino acid  
174 sequence alignment was then used to construct a phylogenetic tree via RAxML<sup>51</sup> (version 8.2.8)  
175 using the substitution model ‘PROTCATWAGF’ (WAG substitution Matrix and empirical base  
176 frequencies) and 100 non-parametric bootstraps. An additional tree was constructed using the  
177 new RAxML-NG with the model LG+F+R5 and 1000 bootstraps<sup>52</sup> (Suppl. Fig. 2). The trees  
178 were rooted on the split between the monophyletic cyanobacterial sequences and the rest of the  
179 taxa.

180 Sequences of plastid-, mitochondria- and dual-targeted proteins of *A. thaliana* were obtained  
181 from Garg and Gould 2016<sup>33</sup>. All proteins were blasted (diamond blastp, identity cutoff: 25%,  
182 evalue cutoff: 1x10<sup>-10</sup>) against a database of 94 cyanobacterial and 460 alphaproteobacterial  
183 proteomes (Suppl. table 2). All hits meeting the cutoffs were plotted against all proteomes in a  
184 2D binary heatmap. The members of each group were sorted according to phylogenetic trees  
185 from concatenated alignments, while the order of genes was determined by hierarchical  
186 clustering (hclust, method: ‘average’). The intracellular localization of the proteins was color  
187 coded.

188

189 *Identification of nuclear encoded, mitochondria- and plastid-targeted genes*

190 Plastid-targeted proteins were identified by blasting known and manually curated plastid-  
191 targeted proteins from *A. thaliana*<sup>33</sup> against the genome of *C. reinhardtii*, *C. paradoxa* and *P.*  
192 *purpureum* (identity of at least 50%, query coverage of at least 50%, maximum E-value of 1x10<sup>-5</sup>)  
193 or extracted from published proteome data when available<sup>53,54</sup>. To identify mitochondria-  
194 targeted proteins, we blasted all mitochondria-targeted proteins from human, mouse and rat  
195 (according to the IMPI database, marked as “Known mitochondrial”) against the genomes of  
196 the three algae (identity of at least 50%, query coverage of at least 50%, maximum E-value of  
197 1x10<sup>-5</sup>). Sequence logos of the mitochondria- and plastid-targeted proteins were curated  
198 manually by aligning the first 20 amino acids following an F, Y, W or L (according to<sup>31</sup>) and  
199 plotted using Seq2Logo<sup>55</sup>.

200

201 **Results**

202 *Adaptive changes of common photosynthetic pigments upon high-light stress*

203 Plants react in particular to changes in light intensity<sup>58,59</sup>. To analyse the differences that high-  
204 light stress has on the three algae, representing the three major groups (Table 1), we set out to  
205 perform comparative studies. The algae were adapted to growing at 50 mol photons m<sup>-2</sup> s<sup>-1</sup>  
206 under a 12/12 day-night cycle and at 20°C. Through rapid light curves we assessed that at 600  
207 mol photons m<sup>-2</sup> s<sup>-1</sup>, a saturation of the photosystems was reached in all three species (Suppl.  
208 Fig. 2). For the high-light stress treatment, the algae were hence exposed to 600  
209 mol photons m<sup>-2</sup> s<sup>-1</sup> for 1h. For comparison we determined the pigment profiles from cultures  
210 that were either 6h into the night or 6h into the day phase.

211 The glaucophyte *C. paradoxa* shows no significant change in pigment concentration or  
212 composition, neither at night nor after light stress (Fig. 2a). For the red alga *P. purpureum* we  
213 observed only very marginal changes and the concentration of pigments for the samples  
214 collected at night was the highest. Pigment concentrations seemed to slowly decrease during  
215 the day and even further under high-light stress. This was observed for all three major pigment  
216 groups at a similar rate (Fig. 2a). Only in the green alga *C. reinhardtii* the pigment composition  
217 changed significantly especially upon high-light stress (Fig. 2a). Here in particular the  
218 xanthophyll cycle, i.e. the enzyme-driven and reversible conversion of violaxanthin into  
219 zeaxanthin is evident, a component of non-photochemical quenching thought to be absent in  
220 glauco- and rhodophytes<sup>24</sup>. Concentrations of chlorophylls and carotenoids actually increase  
221 under high-light stress in *C. reinhardtii*, demonstrating their de novo synthesis.

222 The thylakoid stacks (grana) of land plants relax under high-light stress in order for the repair  
223 mechanism of the photosystems to properly function<sup>60</sup>. This concerns in particular the  
224 degradation of the D1 protein through the membrane-bound protease FtsH, whose dimerized  
225 size is too large for the space where two thylakoid stacks align<sup>59</sup>. Algae form different types of  
226 thylakoid stacks<sup>60,61</sup>, but no grana-like structures. We performed trans-electron microscopy  
227 (TEM)-based analysis of the cells from the three different conditions and determined the  
228 distance between neighbouring thylakoid stacks. The differences we observed were in all cases  
229 marginal, but only in the case of *C. reinhardtii* did we observe a statistically significant increase  
230 in spacing upon high-light stress (Fig. 2b).

231

232 *The transcriptional response to high-light stress is most pronounced in the chlorophyte*

233 We also generated RNA-Seq data on all samples. They reveal stark differences among the three  
234 species in terms of overall transcriptional regulation (Fig. 3). In the chlorophyte, the response  
235 to high-light stress was the most pronounced among the three algae, both regarding the number  
236 of differentially expressed genes as well as in the number of upregulated genes during high-  
237 light conditions. For each condition a clear separation was observed and a specific gene set  
238 upregulated in comparison to the average (Fig. 3).

239 Under high-light conditions the chlorophyte upregulates the expression of photosynthesis  
240 machinery components as well as proteins that promote photoprotection. A total of 418  
241 transcripts were found to be differentially expressed, 274 values of which were significant  
242 (Suppl. table 3). The upregulated photoprotective proteins include stress-related chlorophyll

243 binding proteins 1 and 3 involved in energy-dependent quenching to dissipate excess energy<sup>62</sup>,  
244 members of the early-light inducible protein family (Elip), ancestral homologs of the non-  
245 photochemical quenching associated PSBS/LHCSR3 family<sup>65,66</sup>, a CPD photolyase class II that  
246 reverses the formation of pyrimidine dimers that result from the exposure to strong UV  
247 radiation<sup>67</sup>, and chlorophyll b reductases and beta-carotene hydroxylases that prevent over-  
248 excitation of the photosystem and protects the cells from high-light intensities<sup>68,69</sup>. Next to these  
249 photoprotective proteins, photosynthesis house-keeping genes such as PSII Pbs27, Rieske  
250 protein, PSII subunit 28, and several proteins of the LHC superfamily were upregulated as well  
251 as a few stress-response proteins such as the plastidal homolog of DnaJ and other members of  
252 the HSP70 protein family that can form a multichaperone complex together<sup>70</sup> (Suppl. table 3).

253 In the glaucophyte *C. paradoxa*, most of the 1,463 differentially expressed transcripts were  
254 found upregulated during darkness in correspondence to nightly proliferation. The overall  
255 difference between day and night was far more pronounced than day versus high-light and the  
256 difference between light and high-light conditions smaller than in *Chlamydomonas*. Only 26  
257 transcripts were found to be upregulated during high-light conditions (Suppl. table 3). In  
258 comparison to the green alga, fewer proteins involved in photosynthesis regulation and  
259 photoprotection were found to be upregulated during high-light stress but also included several  
260 Elip proteins.

261 The identification of differentially expressed genes in *P. purpureum* posed to be more difficult.  
262 Only 90 transcripts were initially identified, but by lowering the significance cut-off —  
263 according to the standard edgeR protocol — we were able to detect another 980. The expression  
264 profile matches that of *C. paradoxa*, although the number of regulated genes is far smaller. For  
265 the transition from daylight to high-light, a total of 38 transcripts were identified (Suppl. table  
266 3). The most notable proteins that were upregulated during high-light stress was a high-light  
267 inducible protein (Hlip) involved in non-photochemical quenching<sup>71</sup>, and several heat shock  
268 proteins (HSP70). The response to light stress was far weaker than in the other two algae, but  
269 *P. purpureum* might regulate its RNA levels through the extensive use of miRNAs<sup>72</sup> which  
270 could contribute to the lower levels of differentially expressed genes identified.

271 Comparisons of the most highly upregulated proteins of each of the three algae among all  
272 conditions revealed additional differences in light-dependent differential gene expression.  
273 While *C. reinhardtii* upregulates the synthesis of several photosynthesis and plastid-related  
274 proteins during light and high-light conditions, *C. paradoxa* and *P. purpureum* upregulate only  
275 a few. In the case of *C. paradoxa*, the biggest notable difference is the focus on protein  
276 biosynthesis during darkness/night. The 50 most highly upregulated proteins during the night  
277 consist of approx. 90% ribosomal proteins, indicating an increase in overall protein biosynthesis  
278 and proliferation (Suppl. table 4). We observe photosynthesis machinery components as well  
279 as photoprotection components to be among the most upregulated proteins in combination only  
280 in *C. reinhardtii*, illustrating the chlorophyte's more elaborate ability to adapt to differing light  
281 conditions compared to the other two screened algae.

282

283 *The red Toc75 is an Oep80, and Toc75 unique to Chloroplastida*

284 In *Arabidopsis*, most members of its Toc75 family have been characterized. This includes the  
285 main import pore of the outer membrane, Toc75<sup>73</sup> (TOC75-III, At3g46740), as well as Oep80  
286 (TOC75-V, At5g19620) whose exact function remains unresolved while the protein is essential  
287 for plant viability<sup>74,75</sup>, and most recently SP2 (At3g44160) which serves protein export for  
288 chloroplast-associated protein degradation<sup>76</sup>. The situation in rhodophytes and glaucophytes  
289 differs and they seem not to encode the same number of Toc75 homolog<sup>27,77</sup>.

290 We collected 77 eukaryotic proteins of the Toc75 and Oep80 family from 44 eukaryotic species  
291 and routed them against their cyanobacterial homologs for the construction of a phylogenetic  
292 tree. The single glaucophyte sequence sits basal to all others, while the rhodophyte sequences  
293 form a well-supported group that is sister to all chloroplastidal sequences (Fig. 4). The  
294 sequences of green algae and plants fall into two distinct and again well-supported clusters: one  
295 comprises a group of proteins including the *At*Oep80, the other a group containing the main  
296 import pore *At*Toc75. Within these two groups separating the Oep80 from the Toc75 proteins,  
297 the separation between the chloro- and streptophytes is observed, as well as the basal branching  
298 of *Chara braunii* – a streptophyte alga related to the ancestor of land plants<sup>78,79</sup> (Fig. 4).

299

## 300 **Discussion**

301 If one measures evolutionary success by species diversity, the green lineage is the most  
302 successful. About 16,000 green algal, 5,000 rhodophyte and thirteen glaucophyte species have  
303 been recognized (with >100,000, 500–1000 and about a dozen that remain to be described,  
304 respectively)<sup>80</sup>. Another 400,000 land plant species<sup>81</sup> evolved since the conquering of land some  
305 480 million years ago<sup>82,83</sup>. We argue that the evolutionary origin and success of the green  
306 lineage hinges upon early changes in plastid protein targeting.

307 Algae and plant cells target more than a thousand proteins specifically to each of their two  
308 compartments of endosymbiotic origin. Plastid targeting evolved in a cell that had already  
309 established mitochondrial targeting, yet both import machineries share similarities and both  
310 rely on specific NTSs for matrix and stroma targeting<sup>5</sup>. The origin of the mitochondrial NTS is  
311 uncertain, but its positive charge was an early requirement to overcome the bioenergetic inner  
312 mitochondrial membrane<sup>10</sup>. The most N-terminal domain carries the charged residues critical  
313 for distinguishing between mitochondrial- and plastid targeting (Fig. 1), while the C-terminus  
314 is exchangeable<sup>84</sup>. Because the plastid is younger and because the photosynthetic organelle  
315 evolved in a eukaryotic cell instead of contributing to its actual origin, we understand more  
316 about the origin of the plastid NTS.

317

### 318 *On the origin of the N-terminal targeting sequence*

319 It has been speculated that N-terminal targeting sequences evolved from antimicrobial peptides  
320 (AMPs)<sup>85</sup>, as both share similarities in terms of charged amino acid residues, the ability to form  
321 amphiphilic  $\alpha$ -helices, and because they are frequently identified in host-endosymbiont  
322 relationships<sup>86</sup>. One example regarding the latter is *Paulinella chromatophora*, whose  
323 chromatophore origin is independent from that of the Archaeplastida and younger<sup>87</sup>. Two types  
324 of NTSs were identified that target nuclear-encoded proteins to the chromatophore, but both  
325 are not related to the simultaneously identified AMPs<sup>88</sup>, which argues against an AMP-origin

326 of the NTS in *Paulinella*. The concept is also not compatible with the origin of phenylalanine-  
327 based plastid targeting and Toc75.

328 The components of the Toc and Tic machinery share a mixed pro- and eukaryotic ancestry<sup>89,90</sup>.  
329 Toc75, the β-barrel import pore in the outer membrane, is of prokaryotic origin and a member  
330 of the Omp85 superfamily<sup>25</sup>. Some bacterial Omp85's recognize their substrates through a C-  
331 terminal phenylalanine<sup>91</sup> and evidence is emerging that the POTRA domains of Toc75 act as  
332 binding sites for the NTS<sup>92</sup>. If we recall that the phenylalanine-based motif is retained in  
333 rhodophytes and glaucophytes<sup>29</sup>, we can conclude that the pNTS did not evolve from AMPs  
334 but rather adapted in evolution and traces back to a recognition signal for the cyanobacterial  
335 Omp85 that evolved into Toc75<sup>93</sup>. The ancestral character of phenylalanine-based plastid  
336 targeting was lost with the origin of the Chloroplastida and we suggest simultaneously to the  
337 expansion of the Toc75 family – with significant consequences for the green lineage.

338

339 *Dual-targeting using a single ambiguous signal is the consequence of losing the F-based*  
340 *motif*

341 The use of a F-based motif offered an elegant solution to the archaeoplastidial ancestor. It utilized  
342 an existing translocons-substrate recognition mechanism and allowed to distinguish  
343 cytosolically translated mitochondrial from plastid proteins through a single amino acid-based  
344 motif. With the emergence of the green Toc75 and loss of the F-based motif, false targeting  
345 likely increased. One counter-measure was the increase in phosphorylation sites in the NTS,  
346 which adds negative charge and hampers import of the substrate by mitochondria<sup>10,34,40</sup>. Many  
347 proteins, however, remain dually targeted in *Arabidopsis*<sup>36</sup> and we predict this is restricted to  
348 the green lineage. Dual-targeting to mitochondrion and plastid does occur in algae with a red  
349 plastid, but through alternative transcription/translation initiation and not through the use of a  
350 single ambiguous NTSs<sup>94</sup>.

351 Evolution is blind. Dual-targeting evolves from falsely targeted proteins that initially might not  
352 offer a direct benefit, but are also not detrimental to the cell's viability. This can re-localise or  
353 establish entire new pathways<sup>95</sup> and there is no apparent preference regarding the direction of  
354 flow: as much proteins of cyanobacterial origin are targeted to the mitochondria as they are *vice*  
355 *versa* (Fig. 5). Dual-targeted proteins are largely part of the transcription and translation  
356 machinery<sup>36</sup>. This might include the plastid-associated polymerases, whose dual-targeting in  
357 Chloroplastida might be an ancestral trade of the lineage<sup>79</sup>. Both the mitochondrion and plastid  
358 have a genome, and as such information processing proteins suit a dual-targeting route well. A  
359 simultaneous control over the transcription and translation of both organelles might allow for a  
360 faster and accurate response or simply easier house-keeping. Dual-targeting reinforces the  
361 cross-communication between the two organelles of endosymbiotic origin, likely offering an  
362 evolutionary advantage to cells carrying dozens of mitochondria and plastids simultaneously  
363 such as the cells of land plants but not all algae.

364

365 *An Oep80 derived Toc75 is unique to the green lineage*

366 One of the earliest descriptions of Toc75 was for a protein isolated from pea<sup>96</sup>. Conserved  
367 homologs across all Chloroplastida were quickly identified<sup>15,97</sup>, but required way more effort

368 across the diversity of the Archaeplastida. Through the identification of a Omp85 homolog in  
369 algae with secondary red plastids, it became evident that all phototrophic eukaryotes harbour  
370 beta-barrel forming proteins of an extended Omp85 family that form the import pore in the  
371 outer plastid membrane<sup>98</sup>, but with a decisive difference regarding the number of encoded  
372 homologs.

373 Our phylogenetic analysis of Toc75 and Oep80 supports previous analyses without the need of  
374 any sequence trimming. It demonstrates the clear-cut, likely also functional, separation between  
375 the Toc75 and Oep80 proteins of Chloroplastida<sup>25</sup>. The red sequences are closer to their  
376 prokaryotic homologs and the green Toc75 is further derived. From the perspective of  
377 phylogeny, there is little doubt that Toc75 is unique to the green lineage and originated from  
378 the duplication of an ancestral Omp80 that remains conserved in the other two lineages. This  
379 suggests a division of labour at the outer chloroplast membrane not found in rhodoplasts or  
380 cyanelles, the benefits of which are plenty. Glauco- and rhodophytes work with a single import  
381 pore, whereas *Arabidopsis* and its green relatives encode a single full-length Toc75 and a single  
382 full-length Oep80. Both of the latter are expressed at high levels in a conserved ratio and in the  
383 different tissues according to the gene expression atlas of the TAIR database<sup>99</sup>. Their presence  
384 is needed simultaneously and appears synchronized.

385 We speculate that the duplication of Oep80 allows for a more efficient, faster and versatile  
386 protein import. It might be a prerequisite for the elaborate response to high-light stress, which  
387 our data supports (Fig. 2, Fig. 3). A response to high-light stress is evident in all three lineages  
388 (Fig. 3), but differs in quantity and detail. *Chlamydomonas* not only alters its gene expression  
389 network the most upon high-light stress, but also focuses more on photosynthesis maintenance  
390 and protection, reacts less stressed and rapidly synthesizes pigments de-novo (Fig. 2). The  
391 upregulation of Elips that are of cyanobacterial origin occurs in all three lineages, but they were  
392 only expanded and diversified in the green lineage<sup>100</sup>. Retrograde signalling (a critical part of  
393 the response to high-light stress) is limited by the plastid's import capacity<sup>101</sup>, highlighting the  
394 direct dependence.

395 If Oep80's main duty is indeed the integration of beta-barrel proteins (and maybe other delicate  
396 substrates of unknown nature), then it releases Toc75 from this job. This mirrors the situation  
397 in mitochondria, where Tom40 acts as the main import pore while Sam50 incorporates beta-  
398 barrel proteins with a complicated topology into the outer plastid membrane<sup>102</sup>. The division of  
399 labour appears more effective than the simple increase in number of a single import gateway.  
400 This then maybe also allowed the endosymbiotic gene transfer of the small subunit of RubisCo  
401 to the nucleus, a trademark of the green lineage<sup>103,104</sup>. The sheer amount of RbcS protein  
402 required to be imported might simply overstrain the Oep80 of rhodo- and glaucophytes and its  
403 gene transfer from the plastid to the nucleus is hence selected against. These patterns allow to  
404 speculate on the sequence of evolutionary events.

405 Initially a duplication of the ancestral import pore Oep80 occurred and both paralogs might  
406 have performed the same duty early on. Mutations in one of the two copies led to an  
407 independence of F-based targeting, alternative substrate recognition, the emergence of NTS  
408 phosphorylation<sup>33</sup>, and a cytosolic 14-3-3/Hsp70-based guidance complex<sup>105</sup> that we predict is  
409 unique to the green lineage, too. The plastid-encoded Tic214(YCF1)/YCF2/FtsHi complex  
410 emerged early in chlorophyte evolution, too, maybe through the duplication of an early Tic20-

411 like protein<sup>26,106</sup>. The components of this complex are highly diverse, except for a C-terminal  
412 motif, and were entirely lost in grasses without impacting protein import<sup>107,108</sup>. Other  
413 components were added such as Tic40 that increases import efficiency<sup>109</sup>, and which is absent  
414 from rhodo- and glaucophytes<sup>15</sup>. Ever more plastid proteins went via the Toc75 route, apart  
415 from the slow folding proteins of the outer-membrane that continued to be integrated via Oep80.  
416 A more recent extension was the emergence of the CHLORAD pathway (chloroplast-associated  
417 protein degradation). Its central component, SP2, is an Omp85 paralog as well but lacks the  
418 POTRA domains<sup>76</sup>. It likely emerged in angiosperms and might facilitate the remodelling of  
419 plastids (e.g. of a chloro- to a chromoplast), a feature unique to higher land plants and their  
420 embryoplast<sup>18</sup>. Therefore, the implementation of another plastid protein transport pathway  
421 based on an Oep80 duplication coincided with yet another major step in land plant evolution.

## 422 423 Conclusion

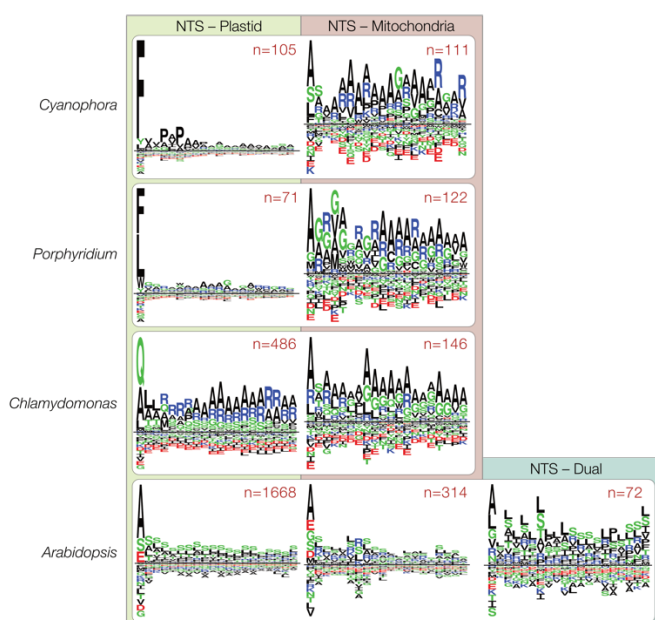
424 Plastid endosymbiosis introduced phototrophs to the eukaryotic tree of life. A critical step was  
425 the evolution of a basic Toc/Tic protein import machinery that is conserved across all algae and  
426 plants. It is evident that major modifications of the Tic/Toc machinery and changes in the  
427 targeting sequences occurred early in the origin of the Chloroplastida. This concerns especially  
428 (i) the loss of phenylalanine-based targeting and (ii) the emergence of new import machinery  
429 components such as Tic40, a plastid-encoded Tic214, and a Toc75 that evolved from the  
430 duplication of the ancestral Omp80. We speculate that the former resulted in the emergence of  
431 dual organelle (plastid and mitochondrion) targeting using a single ambiguous targeting  
432 sequence and that the latter introduced a “high-throughput” import pathway for nuclear-  
433 encoded proteins. The main import pore of the green plastid, Toc75, is released from dealing  
434 with slow-folding proteins of the outer membrane and no longer left hamstrung when there is  
435 the need for rapid import of proteins required to cope with high-light stress. Whatever the details  
436 regarding the substrates imported by Oep80, the Chloroplastida make use of two major import  
437 pores, where rhodophytes and glaucophytes need to cope with one. Responses to high-light  
438 stress is variegated, but it requires the efficient and immediate import of over a hundred nuclear-  
439 encoded plastid proteins simultaneously after retrograde plastid signaling. This was realized by  
440 the implementation of an efficient plastid import pathway that enabled the evolutionary success  
441 of the Chloroplastida, a pinnacle of which was the conquer of land.

## 442 443 444 Acknowledgments

445 We thank Matheus Sanita Lima for discussing dual targeting and Prof. Peter Jahns for providing  
446 access to the HPLC and help in analyzing the pigment profiles. This work was supported  
447 through the DFG (267205415 – SFB 1208) and the VolkswagenStiftung (Life).

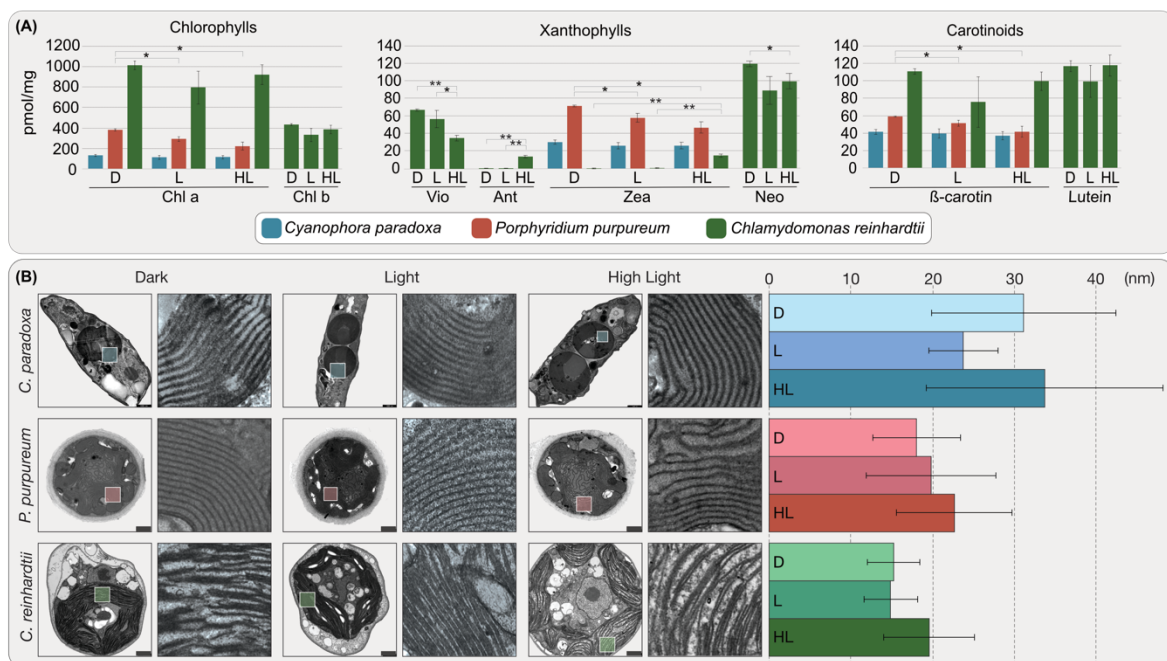
448

449 **Figures**



450

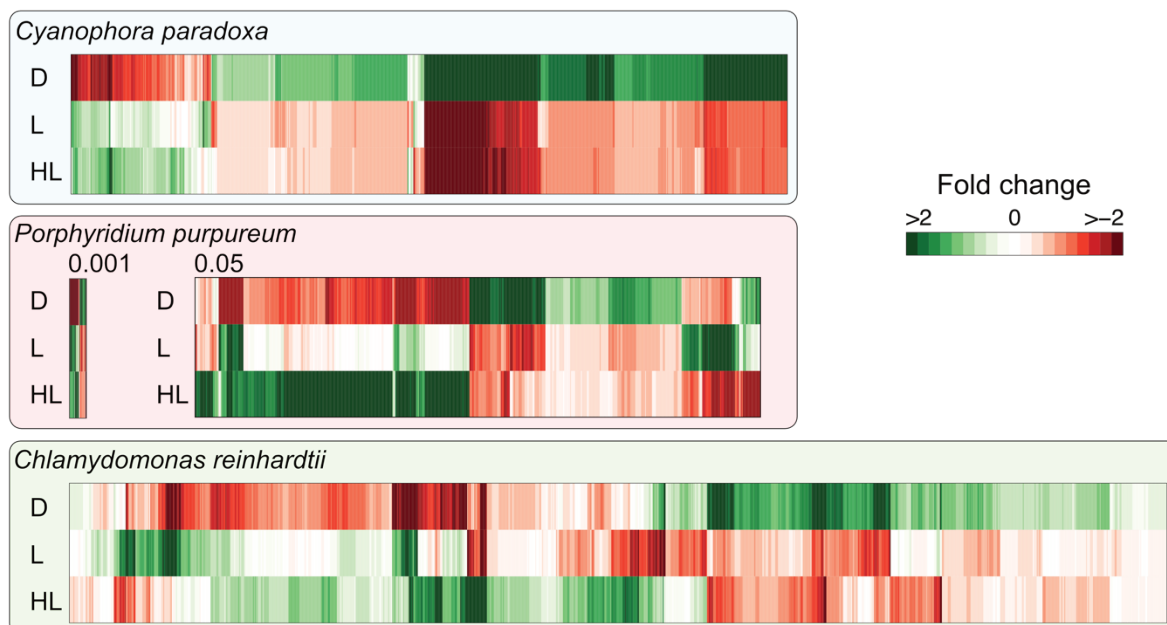
451 **Fig. 1: Targeting motifs and phylogenetic origin of organelle targeted proteins. (a)** NTS of  
452 plastid- or mitochondria-targeted proteins of *C. paradoxa*, *C. merolae* and *A. thaliana*. The  
453 three species showcase the NTS for plastid- or mitochondria-targeting in the *Glauco*phyta,  
454 *Rhodophyta* and *Chlorophyta*, respectively. While an F-based plastid targeting motif is evident  
455 in *Glauco*phyta and *Rhodophyta*, it was lost in the green lineage.



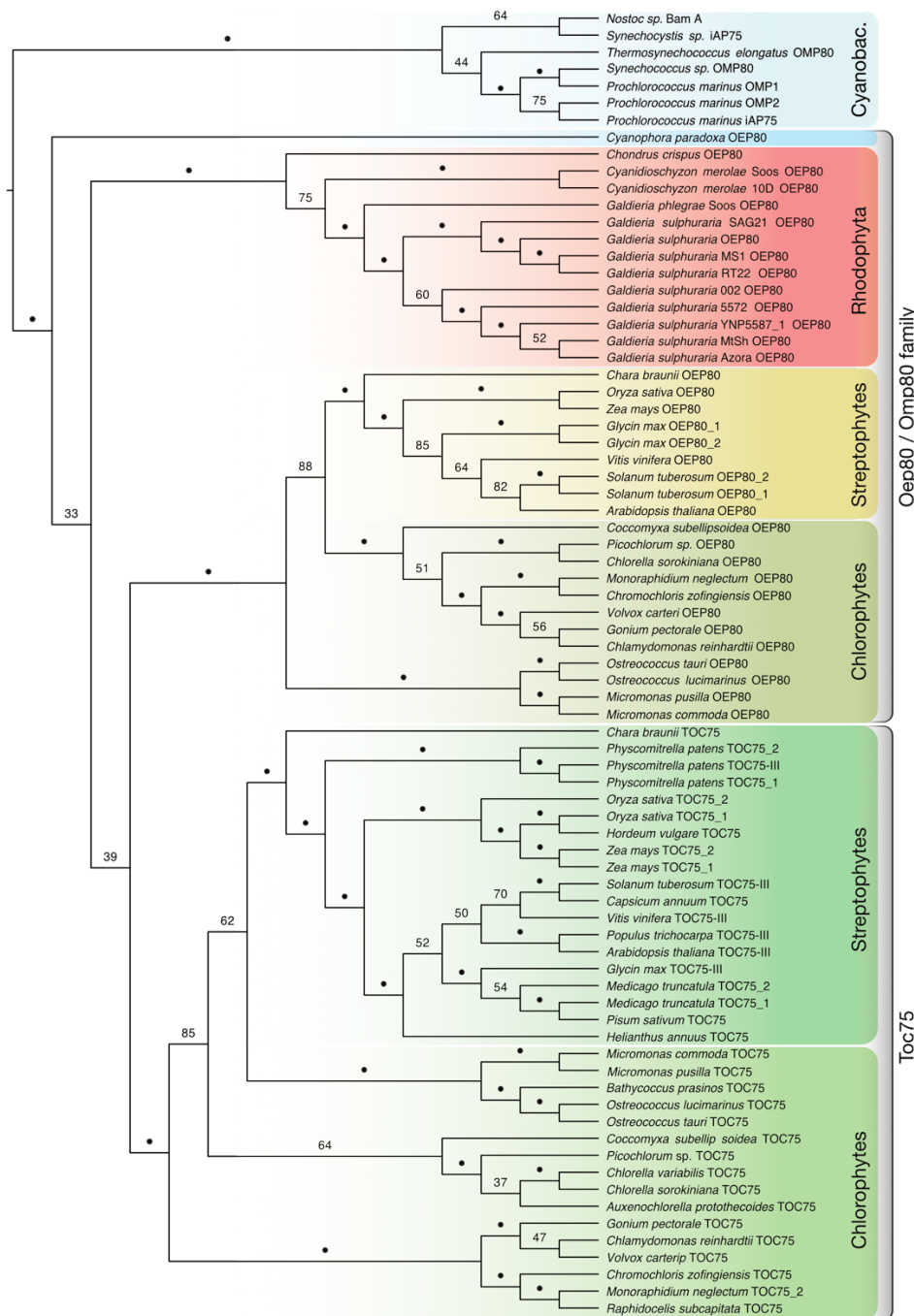
456

457 **Fig. 2: Pigment profiles and analysis of thylakoid stack distance during high-light stress.**  
458 (a) Pigments were extracted by homogenization with acetone and their concentrations  
459 determined by an HPLC analysis. In both the glaucophyte and rhodophyte the pigment  
460 concentrations remain rather stable and only a slight decrease in the overall pigment  
461 concentration is observed during the day and even more so during high-light stress. On the

462 contrary, in *C. reinhardtii* all three types of pigment change their concentration significantly  
463 and e.g. the step-wise reduction of violaxanthin (Vio) to antheraxanthin (Ant) and zeaxanthin  
464 (zea) is evident. **(b)** Cells from the three different conditions were fixed and analyzed using  
465 trans-electron microscopy and distances between the thylakoids were measured using Fiji. An  
466 obvious and statistically significant increase in thylakoid distance upon high-light stress is only  
467 observed in *C. reinhardtii*, although a similar but less significant trend is observed in the red  
468 alga *P. purpureum*. \* $<0,05$     \*\* $<0,001$     \*\*\* $<0,0001$

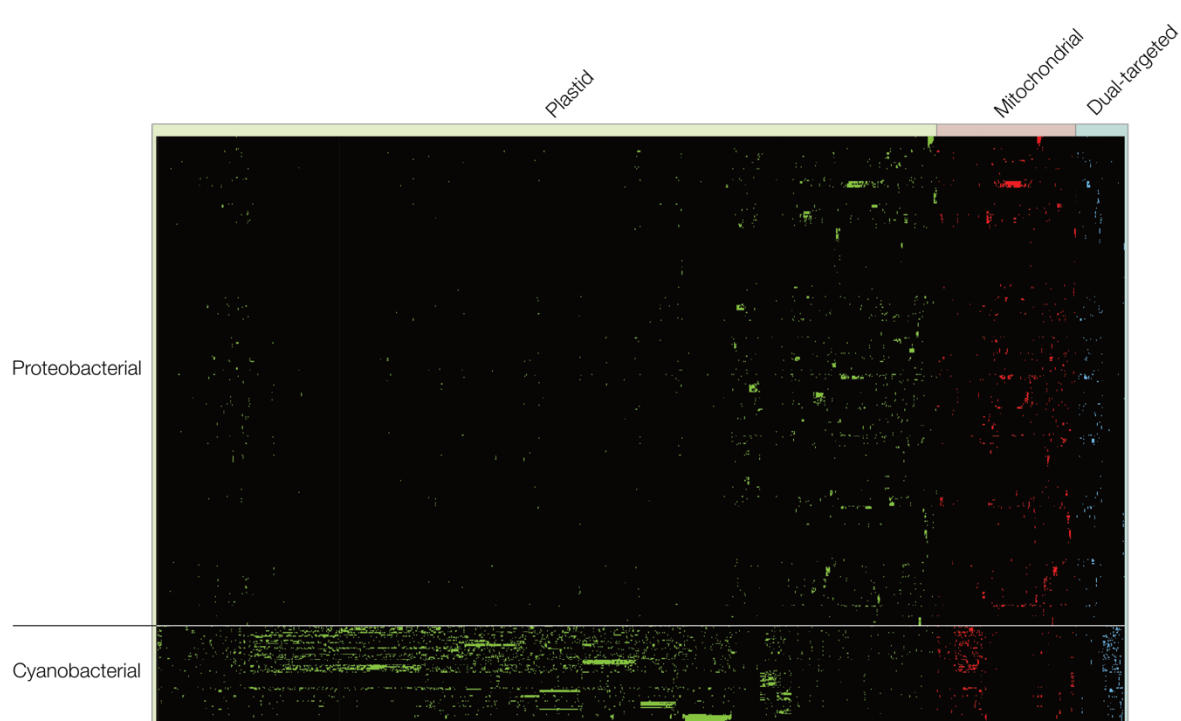


469  
470 **Fig. 3: Differentially expressed genes of *C. reinhardtii*, *C. paradoxa* and *P. purpureum*.**  
471 Visualization of all differentially expressed genes of *C. reinhardtii*, *C. paradoxa* and *P.*  
472 *purpureum*, colored according to the logarithmic fold change of the expression among all tested  
473 light conditions. Logarithmic fold changes of gene expression are color coded. For *C.*  
474 *reinhardtii* and *C. paradoxa*, the fold change's significance of all visualized transcripts is at  
475 least 0.001. For *P. purpureum*, the significance cutoff was lowered to 0.05, since the original  
476 cutoff revealed only 90 differentially expressed genes. *C. reinhardtii* shows distinct sets of  
477 genes each tailored towards one of the tested light conditions. *C. paradoxa* and *P. purpureum*  
478 on the other hand, do not show such an adaptation to altering light conditions, especially not to  
479 high-light. *C. paradoxa* does not change much of its gene expression between daylight and  
480 high-light conditions, showing its lack of adaptation. Although *P. purpureum* expresses a set  
481 of genes only during high-light conditions, their differential expression was only detectable by  
482 lowering the significance cutoff. Even if all differentially expressed genes of *P. purpureum* are  
483 considered, its transcriptional changes during high-light remain minor.



484

485 **Fig. 4: Phylogenetic analysis of Oep80 and Toc75 homologs.** A total of 77 amino acid  
 486 sequences of Oep80/Toc75 homologs from members of the chlorophytes, rhodophytes and  
 487 glaucophytes were used for phylogeny reconstruction via RAxML (PROTCATWAGF) with  
 488 100 bootstraps. The tree was rooted on the split between the monophyletic cyanobacteria and  
 489 the eukaryotic sequences. The cyanobacteria as well as all three algal groups form  
 490 monophyletic groups. Within the green lineage, the Toc75 and Oep80 sequences form separate  
 491 clusters, indicating the emergence of Toc75 within the green lineage.



492

493 **Fig. 5: Phylogenetic origin of plastid- and mitochondria-targeted proteins of *Arabidopsis*.**  
494 Binary presence and absence pattern of homologs of plastid- (green), mitochondria- (red) and  
495 dual-targeted (blue) proteins of *A. thaliana* within 94 cyanobacterial and 460  
496 alphaproteobacterial proteomes. Organisms are sorted according to previously constructed  
497 group-specific phylogenies, while genes are sorted by hierarchical clustering. Most homologs  
498 of plastid-targeted genes were identified in cyanobacteria, but for more than one fifth (22%) of  
499 the plastid-targeted genes the majority of homologs were identified in alphaproteobacteria. In  
500 the case of mitochondria-targeted genes, for almost one third (35%) of the genes most homologs  
501 were identified in cyanobacteria instead of alphaproteobacteria. The phylogenetic signal of the  
502 dual-targeted genes is more evenly distributed among cyanobacteria and alphaproteobacterial  
503 with one half (45%) showing a cyanobacterial origin and the other half (55%) showing an  
504 alphaproteobacterial origin.

505

506 **Table 1:** Major differences among the three primary algae lineages and land plants, concerning  
507 their coding capacity, composition of the photosynthetic apparatus and carbon storage  
508 properties.

Organism	Protein-coding genes			Antenna proteins	Chlorophylls	Antenna pigments	Thylakoid organization	Starch & Storage
	Nucleus	Plastid	Mitochondrion					
<i>Arabidopsis thaliana</i> ( <i>Streptophyte plant</i> )	35,176	88	122	LHC protein complex	a,b	beta-Carotin, Lutein, Neoxanthin, Violaxanthin, Antheraxanthin, Zeaxanthin	Stacked, Grana	Starch
<i>Chara braunii</i> ( <i>Streptophyte algae</i> )	23,546	105	46	LHC protein complex	a,b	beta-Carotin, Lutein, Neoxanthin, Violaxanthin, Antheraxanthin, Zeaxanthin	Stacked	Starch
<i>Chlamydomonas reinhardtii</i> ( <i>Chlorophyte algae</i> )	14,411	69 <sup>s</sup>	8 <sup>s</sup>	LHC protein complex	a,b	beta-Carotin, Lutein, Neoxanthin, Violaxanthin, Antheraxanthin, Zeaxanthin	Stacked	Starch
<i>Porphyridium purpureum</i> ( <i>Rhodophyte</i> )	8,355	199 <sup>s</sup>	n.d.	Phycobilisomes	a	beta-Carotin, Zeaxanthin	Unstacked, equidistant and single	Glycogen, Floridean starch
<i>Cyanophora paradoxa</i> ( <i>Glaucophyte</i> )	27,921 (25,831)	136 <sup>s</sup>	44 <sup>s</sup>	Phycobilisomes	a	beta-Carotin, Zeaxanthin	Unstacked, equidistant and single	Floridean starch

509

510

## 511 References

1. Zimorski, V., Ku, C., Martin, W. F. & Gould, S. B. Endosymbiotic theory for organelle origins. *Curr. Opin. Microbiol.* **22**, 38–48 (2014).
2. Archibald, J. M. Endosymbiosis and Eukaryotic Cell Evolution. *Curr. Biol.* **25**, R911–R921 (2015).
3. Timmis, J. N., Ayliff, M. A., Huang, C. Y. & Martin, W. Endosymbiotic gene transfer: Organelle genomes forge eukaryotic chromosomes. *Nature Reviews Genetics* **5**, 123–135 (2004).
4. Martin, W. & Herrmann, R. G. Gene Transfer from Organelles to the Nucleus: How Much, What Happens, and Why? *Plant Physiol.* **118**, 9–17 (1998).
5. Schleiff, E. & Becker, T. Common ground for protein translocation: Access control for mitochondria and chloroplasts. *Nature Reviews Molecular Cell Biology* **12**, 48–59 (2011).
6. Dudek, J., Rehling, P. & van der Laan, M. Mitochondrial protein import: Common principles and physiological networks. *Biochimica et Biophysica Acta - Molecular Cell Research* **1833**, 274–285 (2013).
7. Paila, Y. D., Richardson, L. G. L. & Schnell, D. J. New insights into the mechanism of chloroplast protein import and its integration with protein quality control, organelle biogenesis and development. *Journal of Molecular Biology* **427**, 1038–1060 (2015).

530 8. Goldberg, A. V. *et al.* Localization and functionality of microsporidian iron-sulphur  
531 cluster assembly proteins. *Nature* **452**, 624–628 (2008).

532 9. Hamilton, V., Singha, U. K., Smith, J. T., Weems, E. & Chaudhuri, M. Trypanosome  
533 alternative oxidase possesses both an N-terminal and internal mitochondrial targeting  
534 signal. *Eukaryot. Cell* **13**, 539–47 (2014).

535 10. Garg, S. *et al.* Conservation of transit peptide-Independent protein import into the  
536 mitochondrial and hydrogenosomal matrix. *Genome Biol. Evol.* **7**, 2716–2726 (2015).

537 11. Rodríguez-Ezpeleta, N. *et al.* Monophyly of primary photosynthetic eukaryotes: Green  
538 plants, red algae, and glaucophytes. *Curr. Biol.* **15**, 1325–1330 (2005).

539 12. Jackson, C. J. & Reyes-Prieto, A. The mitochondrial genomes of the glaucophytes  
540 gloeochaete wittrockiana and cyanoptyche gloeocystis: Multilocus phylogenetics  
541 suggests a monophyletic archaeoplastida. *Genome Biol. Evol.* **6**, 2774–2785 (2014).

542 13. Sánchez-Baracaldo, P., Raven, J. A., Pisani, D. & Knoll, A. H. Early photosynthetic  
543 eukaryotes inhabited low-salinity habitats. *Proc. Natl. Acad. Sci. U. S. A.* **114**, E7737–  
544 E7745 (2017).

545 14. Cavalier-Smith, T. Principles of protein and lipid targeting in secondary  
546 symbiogenesis: euglenoid, dinoflagellate, and sporozoan plastid origins and the  
547 eukaryote family tree. *J. Eukaryot. Microbiol.* **46**, 347–66 (1999).

548 15. Kalanon, M. & McFadden, G. I. The chloroplast protein translocation complexes of  
549 *Chlamydomonas reinhardtii*: A bioinformatic comparison of Toc and Tic components  
550 in plants, green algae and red algae. *Genetics* **179**, 95–112 (2008).

551 16. Gould, S. B., Maier, U. G. & Martin, W. F. Protein Import and the Origin of Red  
552 Complex Plastids. *Current Biology* **25**, R515–R521 (2015).

553 17. Gibson, T. M. *et al.* Precise age of *Bangiomorpha pubescens* dates the origin of  
554 eukaryotic photosynthesis. *Geology* **46**, (2017).

555 18. de Vries, J., Stanton, A., Archibald, J. M. & Gould, S. B. Streptophyte  
556 Terrestrialization in Light of Plastid Evolution. *Trends in Plant Science* **21**, 467–476  
557 (2016).

558 19. Pfanzagl, B. *et al.* Primary structure of cyanelle peptidoglycan of Cyanophora  
559 paradoxa: A prokaryotic cell wall as part of an organelle envelope. *J. Bacteriol.* **178**,  
560 332–339 (1996).

561 20. Hirano, T. *et al.* Moss chloroplasts are surrounded by a peptidoglycan wall containing  
562 D-amino acids. *Plant Cell* **28**, 1521–1532 (2016).

563 21. Suzuki, E. & Suzuki, R. Variation of Storage Polysaccharides in Phototrophic  
564 Microorganisms. *J. Appl. Glycosci.* **60**, 21–27 (2013).

565 22. Allen, D. K., Laclair, R. W., Ohlrogge, J. B. & Shachar-Hill, Y. Isotope labelling of  
566 Rubisco subunits provides *in vivo* information on subcellular biosynthesis and  
567 exchange of amino acids between compartments. *Plant, Cell Environ.* **35**, 1232–1244  
568 (2012).

569 23. Tomitani, A. *et al.* Chlorophyll b and phycobilins in the common ancestor of  
570 cyanobacteria and chloroplasts. *Nature* **400**, 159–162 (1999).

571 24. Goss, R. & Jakob, T. Regulation and function of xanthophyll cycle-dependent  
572 photoprotection in algae. *Photosynthesis Research* **106**, 103–122 (2010).

573 25. Day, P. M., Potter, D. & Inoue, K. Evolution and targeting of *omp85* homologs in the

574 chloroplast outer envelope membrane. *Front. Plant Sci.* **5**, (2014).

575 26. Kikuchi, S. *et al.* Uncovering the protein translocon at the chloroplast inner envelope  
576 membrane. *Science*. **339**, 571–574 (2013).

577 27. Köhler, D. *et al.* Identification of protein N-termini in Cyanophora paradoxa cyanelles:  
578 Transit peptide composition and sequence determinants for precursor maturation.  
579 *Front. Plant Sci.* **6**, 1–11 (2015).

580 28. Steiner, J. M., Yusa, F., Pompe, J. A. & Löffelhardt, W. Homologous protein import  
581 machineries in chloroplasts and cyanelles. *Plant J.* (2005). doi:10.1111/j.1365-  
582 313X.2005.02559.x

583 29. Wunder, T., Martin, R., Löffelhardt, W., Schleiff, E. & Steiner, J. M. The invariant  
584 phenylalanine of precursor proteins discloses the importance of Omp85 for protein  
585 translocation into cyanelles. *BMC Evol. Biol.* **7**, (2007).

586 30. Gruber, A. *et al.* Protein targeting into complex diatom plastids: Functional  
587 characterisation of a specific targeting motif. *Plant Mol. Biol.* **64**, 519–530 (2007).

588 31. Patron, N. J. & Waller, R. F. Transit peptide diversity and divergence: A global  
589 analysis of plastid targeting signals. *BioEssays* **29**, 1048–1058 (2007).

590 32. Garg, S. G. & Gould, S. B. The Role of Charge in Protein Targeting Evolution. *Trends  
591 in Cell Biology* **26**, 894–905 (2016).

592 33. Lee, J., O'Neill, R. C., Park, M. W., Gravel, M. & Braun, P. E. Mitochondrial  
593 localization of CNP2 is regulated by phosphorylation of the N-terminal targeting signal  
594 by PKC: Implications of a mitochondrial function for CNP2 in glial and non-glial cells.  
595 *Mol. Cell. Neurosci.* **31**, 446–462 (2006).

596 34. Karniely, S. & Pines, O. Single translation-dual destination: Mechanisms of dual  
597 protein targeting in eukaryotes. *EMBO Reports* **6**, 420–425 (2005).

598 35. Carrie, C. & Small, I. A reevaluation of dual-targeting of proteins to mitochondria and  
599 chloroplasts. *Biochim. Biophys. Acta - Mol. Cell Res.* **1833**, 253–259 (2013).

600 36. Carrie, C. *et al.* Approaches to defining dual-targeted proteins in Arabidopsis. *Plant J.*  
601 **57**, 1128–1139 (2009).

602 37. Chew, O. *et al.* A plant outer mitochondrial membrane protein with high amino acid  
603 sequence identity to a chloroplast protein import receptor. *FEBS Lett.* **557**, 109–14  
604 (2004).

605 38. Sun, F. *et al.* AtPAP2 is a tail-anchored protein in the outer membrane of chloroplasts  
606 and mitochondria. *Plant Signal. Behav.* **7**, (2012).

607 39. Law, Y.-S. *et al.* Phosphorylation and Dephosphorylation of the Presequence of  
608 Precursor MULTIPLE ORGANELLAR RNA EDITING FACTOR3 during Import into  
609 Mitochondria from Arabidopsis. *Plant Physiol.* **169**, 1344–55 (2015).

610 40. Gould, S. B. *et al.* Adaptation to life on land at high O<sub>2</sub> via transition from ferredoxin-  
611 to NADH-dependent redox balance. *Proc. R. Soc. B Biol. Sci.* **286**, 20191491 (2019).

612 41. Grabherr, M. G. *et al.* Full-length transcriptome assembly from RNA-Seq data without  
613 a reference genome. *Nat. Biotechnol.* **29**, 644–652 (2011).

614 42. Robinson, M. D., McCarthy, D. J. & Smyth, G. K. edgeR: A Bioconductor package for  
615 differential expression analysis of digital gene expression data. *Bioinformatics* **26**, 139–  
616 140 (2009).

617 43. O'Leary, N. A. *et al.* Reference sequence (RefSeq) database at NCBI: Current status,  
618 taxonomic expansion, and functional annotation. *Nucleic Acids Res.* **44**, D733–D745  
619 (2016).

620 44. Clark, K., Karsch-mizrachi, I., Lipman, D. J., Ostell, J. & Sayers, E. W. GenBank.  
621 *Nucleic Acids Res.* **44**, 67–72 (2016).

622 45. Inoue, K. & Potter, D. The chloroplastic protein translocation channel Toc75 and its  
623 paralog OEP80 represent two distinct protein families and are targeted to the  
624 chloroplastic outer envelope by different mechanisms. *Plant J.* **39**, 354–365 (2004).

625 46. Rossoni AW, Price DC, Seger M, Lyska D, Lammers P, Bhattacharya D, Weber AP..  
626 The genomes of polyextremophilic cyanidiales contain 1% horizontally transferred  
627 genes with diverse adaptive functions. *eLife Sciences* **8**, 1283 (2019).

628 47. Grigoriev, I. V *et al.* The Genome Portal of the Department of Energy Joint Genome  
629 Institute. *Nucleic Acids Res.* **40**, 26–32 (2012).

630 48. Altschul, S. F. *et al.* Gapped BLAST and PSI-BLAST: A new generation of protein  
631 database search programs. *Nucleic Acids Research* **25**, 3389–3402 (1997).

632 49. Altschul, S. F., Gish, W., Miller, W., Myers, E. W. & Lipman, D. J. Basic local  
633 alignment search tool. *J. Mol. Biol.* **215**, 403–410 (1990).

634 50. Katoh, K., Misawa, K., Kuma, K. & Miyata, T. MAFFT: a novel method for rapid  
635 multiple sequence alignment based on fast Fourier transform. *Nucleic Acids Res.* **30**,  
636 3059–3066 (2002).

637 51. Stamatakis, A. RAxML version 8: A tool for phylogenetic analysis and post-analysis of  
638 large phylogenies. *Bioinformatics* **30**, 1312–1313 (2014).

639 52. Kozlov, A. M., Darriba, D., Flouri, T., Morel, B. & Stamatakis, A. RAxML-NG: a fast,  
640 scalable and user-friendly tool for maximum likelihood phylogenetic inference.  
641 *Bioinformatics* (2019). doi:10.1093/bioinformatics/btz305

642 53. Terashima M, Specht M, Naumann B, Hippler M.. Characterizing the anaerobic  
643 response of *Chlamydomonas reinhardtii* by quantitative proteomics. *Mol. Cell  
644 Proteomics* **9**, 1514–1532 (2010).

645 54. Facchinelli F, Pribil M, Oster U, Ebert NJ, Bhattacharya D, Leister D, Weber APM.  
646 2013. Proteomic analysis of the Cyanophora paradoxa muroplast provides clues on  
647 early events in plastid endosymbiosis. *Planta* 237:637–651.

648 55. Thomsen, M. C. F. & Nielsen, M. Seq2Logo: A method for construction and  
649 visualization of amino acid binding motifs and sequence profiles including sequence  
650 weighting, pseudo counts and two-sided representation of amino acid enrichment and  
651 depletion. *Nucleic Acids Res.* **40**, W281–W287 (2012).

652 56. Färber, A., Young, A. J., Ruban, A. V., Horton, P. & Jahns, P. Dynamics of  
653 Xanthophyll-Cycle Activity in Different Antenna Subcomplexes in the Photosynthetic  
654 Membranes of Higher Plants (The Relationship between Zeaxanthin Conversion and  
655 Nonphotochemical Fluorescence Quenching). *Plant Physiol.* **115**, 1609–1618 (1997).

656 57. Schindelin, J. *et al.* Fiji: An open-source platform for biological-image analysis. *Nature  
657 Methods* **9**, 676–682 (2012).

658 58. Lichtenthaler, H. K. *et al.* Photosynthetic activity, chloroplast ultrastructure, and leaf  
659 characteristics of high-light and low-light plants and of sun and shade leaves.  
660 *Photosynth. Res.* **2**, 115–141 (1981).

661 59. Zhu, J. K. Abiotic Stress Signaling and Responses in Plants. *Cell* **167**, 313–324 (2016).

662 60. Khatoon, M. *et al.* Quality control of photosystem II: Thylakoid unstacking necessary  
663 to avoid further damage to the D1 protein and to facilitate D1 degradation under light  
664 stress in spinach thylakoids. *J. Biol. Chem.* **284**, 25343–25352 (2009).

665 61. Yoshioka-Nishimura, M. & Yamamoto, Y. Quality control of Photosystem II: The  
666 molecular basis for the action of FtsH protease and the dynamics of the thylakoid  
667 membranes. *Journal of Photochemistry and Photobiology B: Biology* **137**, 100–106  
668 (2014).

669 62. Bertrand, M. Carotenoid biosynthesis in diatoms. *Photosynthesis Research* **106**, 89–  
670 102 (2010).

671 63. Tsekos, I., Reiss, H. D., Orfanidis, S. & Orologas, N. Ultrastructure and  
672 supramolecular organization of photosynthetic membranes of some marine red algae.  
673 *New Phytol.* **133**, 543–551 (1996).

674 64. Bonente, G. *et al.* Analysis of LHcSR3, a protein essential for feedback de-excitation  
675 in the green alga *Chlamydomonas reinhardtii*. *PLoS Biol.* **9**, e1000577 (2011).

676 65. Hutin, C. *et al.* Early light-induced proteins protect *Arabidopsis* from photooxidative  
677 stress. *Proc. Natl. Acad. Sci. U. S. A.* **100**, 4921–4926 (2003).

678 66. Engelken, J., Brinkmann, H. & Adamska, I. Taxonomic distribution and origins of the  
679 extended LHC (light-harvesting complex) antenna protein superfamily. *BMC Evol.  
680 Biol.* **10**, (2010).

681 67. Carell, T., Burgdorf, L. T., Kundu, L. M. & Cichon, M. The mechanism of action of  
682 DNA photolyases. *Current Opinion in Chemical Biology* **5**, 491–498 (2001).

683 68. Sato, R., Ito, H. & Tanaka, A. Chlorophyll b degradation by chlorophyll b reductase  
684 under high-light conditions. *Photosynth. Res.* **126**, 249–59 (2015).

685 69. Davison, P. A., Hunter, C. N. & Horton, P. Overexpression of  $\beta$ -carotene hydroxylase  
686 enhances stress tolerance in *Arabidopsis*. *Nature* **418**, 203–206 (2002).

687 70. Willmund, F., Dorn, K. V., Schulz-Raffelt, M. & Schroda, M. The chloroplast DnaJ  
688 homolog CDJ1 of *Chlamydomonas reinhardtii* is part of a multichaperone complex  
689 containing HSP70B, CGE1, and HSP90C. *Plant Physiol.* **148**, 2070–2082 (2008).

690 71. Komenda, J. & Sobotka, R. Cyanobacterial high-light-inducible proteins - Protectors of  
691 chlorophyll-protein synthesis and assembly. *Biochim. Biophys. Acta - Bioenerg.* **1857**,  
692 288–295 (2016).

693 72. Gao, F. *et al.* Identification of conserved and novel microRNAs in *Porphyridium  
694 purpureum* via deep sequencing and bioinformatics. *BMC Genomics* **17**, (2016).

695 73. Kessler, F., Blobel, G., Patel, H. A. & Schnell, D. J. Identification of two GTP-binding  
696 proteins in the chloroplast protein import machinery. *Science (80-. ).* **266**, 1035–1039  
697 (1994).

698 74. Hsu, S.-C., Patel, R., Bédard, J., Jarvis, P. & Inoue, K. Two distinct Omp85 paralogs in  
699 the chloroplast outer envelope membrane are essential for embryogenesis in  
700 *Arabidopsis thaliana*. *Plant Signal. Behav.* **3**, 1134–5 (2008).

701 75. Patel, R., Hsu, S. C., Bédard, J., Inoue, K. & Jarvis, P. The Omp85-related chloroplast  
702 outer envelope protein OEP80 is essential for viability in *Arabidopsis*. *Plant Physiol.*  
703 **148**, 235–245 (2008).

704 76. Ling, Q. *et al.* Ubiquitin-dependent chloroplast-associated protein degradation in

705 plants. *Science* (80-). **363**, (2019).

706 77. Töpel, M., Ling, Q. & Jarvis, P. Neofunctionalization within the Omp85 protein  
707 superfamily during chloroplast evolution. *Plant Signal. Behav.* **7**, (2012).

708 78. Wickett, N. J. *et al.* Phylogenomic analysis of the origin and early diversification  
709 of land plants. *Proc. Natl. Acad. Sci. U. S. A.* **111**, E4859–E4868 (2014).

710 79. Nishiyama, T. *et al.* The Chara Genome: Secondary Complexity and Implications for  
711 Plant Terrestrialization. *Cell* **174**, 448-464.e24 (2018).

712 80. Andersen, R. A. Diversity of eukaryotic algae. *Biodivers. Conserv.* **1**, 267–292 (1992).

713 81. Govaerts, R. How many species of seed plants are there? *Taxon* **50**, 1085–1090 (2001).

714 82. Kenrick, P., Wellman, C. H., Schneider, H. & Edgecombe, G. D. A timeline for  
715 terrestrialization: Consequences for the carbon cycle in the Palaeozoic. *Philosophical  
716 Transactions of the Royal Society B: Biological Sciences* **367**, 519–536 (2012).

717 83. Delwiche, C. F. & Cooper, E. D. The evolutionary origin of a terrestrial flora. *Current  
718 Biology* **25**, R899–R910 (2015).

719 84. Lee, D. W. *et al.* Molecular Mechanism of the Specificity of Protein Import into  
720 Chloroplasts and Mitochondria in Plant Cells. *Mol. Plant* **12**, 951–966 (2019).

721 85. Wollman, F. A. An antimicrobial origin of transit peptides accounts for early  
722 endosymbiotic events. *Traffic* **17**, 1322–1328 (2016).

723 86. Mergaert, P., Kikuchi, Y., Shigenobu, S. & Nowack, E. C. M. Metabolic Integration of  
724 Bacterial Endosymbionts through Antimicrobial Peptides. *Trends in Microbiology* **25**,  
725 703–712 (2017).

726 87. Nowack, E. C. M. Paulinella chromatophora - Rethinking the transition from  
727 endosymbiont to organelle. *Acta Societatis Botanicorum Poloniae* **83**, 387–397 (2014).

728 88. Singer, A. *et al.* Massive Protein Import into the Early-Evolutionary-Stage  
729 Photosynthetic Organelle of the Amoeba Paulinella chromatophora. *Curr. Biol.* **27**,  
730 2763-2773.e5 (2017).

731 89. Jarvis, P. & Soll, J. Toc, Tic, and chloroplast protein import. *Biochimica et Biophysica  
732 Acta - Molecular Cell Research* **1541**, 64–79 (2001).

733 90. Day, P. M. & Theg, S. M. Evolution of protein transport to the chloroplast envelope  
734 membranes. *Photosynthesis Research* **138**, 315–326 (2018).

735 91. Robert, V. *et al.* Assembly factor Omp85 recognizes its outer membrane protein  
736 substrates by a species-specific C-terminal motif. *PLoS Biol.* **4**, 1984–1995 (2006).

737 92. O’Neil, P. K. *et al.* The POTRA domains of Toc75 exhibit chaperone-like function to  
738 facilitate import into chloroplasts. *Proc. Natl. Acad. Sci. U. S. A.* **114**, E4868–E4876  
739 (2017).

740 93. Sommer, M. S. *et al.* Chloroplast Omp85 proteins change orientation during evolution.  
741 *Proc. Natl. Acad. Sci. U. S. A.* **108**, 13841–13846 (2011).

742 94. Gile, G. H., Moog, D., Slamovits, C. H., Maier, U. G. & Archibald, J. M. Dual  
743 organellar targeting of aminoacyl-tRNA synthetases in diatoms and cryptophytes.  
744 *Genome Biol. Evol.* **7**, 1728–1742 (2015).

745 95. Martin, W. Evolutionary origins of metabolic compartmentalization in eukaryotes.  
746 *Philosophical Transactions of the Royal Society B: Biological Sciences* **365**, 847–855  
747 (2010).

748 96. Schnell, D. J., Kessler, F. & Blobel, G. Isolation of components of the chloroplast  
749 protein import machinery. *Science* (80- ). **266**, 1007–1012 (1994).

750 97. Shi, L. X. & Theg, S. M. The chloroplast protein import system: From algae to trees.  
751 *Biochimica et Biophysica Acta - Molecular Cell Research* **1833**, 314–331 (2013).

752 98. Bullmann, L. *et al.* Filling the gap, evolutionarily conserved Omp85 in plastids of  
753 chromalveolates. *J. Biol. Chem.* **285**, 6848–6856 (2010).

754 99. Berardini, T. Z. *et al.* The arabidopsis information resource: Making and mining the  
755 “gold standard” annotated reference plant genome. *Genesis* **53**, 474–485 (2015).

756 100. Heddad, M. & Adamska, I. The evolution of light stress proteins in photosynthetic  
757 organisms. *Comp. Funct. Genomics Comp Funct Genom* **3**, 504–510 (2002).

758 101. Wu, G. Z. *et al.* Control of retrograde signalling by protein import and cytosolic  
759 folding stress. *Nat. Plants* **5**, 525–538 (2019).

760 102. Wiedemann, N. *et al.* Machinery for protein sorting and assembly in the mitochondrial  
761 outer membrane. *Nature* **424**, 565–571 (2003).

762 103. Broglie, R., Coruzzi, G., Lamppa, G., Keith, B. & Chua, N. H. Structural Analysis of  
763 Nuclear Genes Coding for the Precursor to the Small Subunit of Wheat Ribulose-1,5-  
764 Bisphosphate Carboxylase. *Bio/Technology* **1**, 55–61 (1983).

765 104. Coen, D. M., Bedbrook, J. R., Bogorad, L. & Rich, A. Maize chloroplast DNA  
766 fragment encoding the large subunit of ribulosebisphosphate carboxylase. *Proc. Natl.  
767 Acad. Sci.* **74**, 5487–5491 (1977).

768 105. May, T. & Soll, J. 14-3-3 Proteins Form a Guidance Complex with Chloroplast  
769 Precursor Proteins in Plants. *Plant Cell* **12**, 53–63 (2000).

770 106. Kikuchi S, Asakura Y, Imai M, Nakahira Y, Kotani Y, Hashiguchi Y, Nakai Y,  
771 Takafuji K, Bédard J, Hirabayashi-Ishioka Y, et al.. A Ycf2-FtsHi heteromeric AAA-  
772 ATPase complex is required for chloroplast protein import. *Plant Cell* tpc.00357.2018–  
773 tpc.00357.2028 (2018).

774 107. de Vries J, Archibald JM, Gould SB. The carboxy terminus of YCF1 contains a motif  
775 conserved throughout >500 million years of streptophyte evolution. *Genome Biol Evol.*  
776 **9**, 473–479 (2017).

777 108. de Vries J, Sousa FL, Böltner B, Soll J, Gould SB. 2015. YCF1: A Green TIC? *Plant  
778 Cell* **27**, 1827–1833 (2015).

779 109. Chou M-L, Fitzpatrick LM, Tu SL, Budziszewski G, Potter-Lewis S, Akita M, Levin  
780 JZ, Keegstra K, Li H-M. Tic40, a membrane-anchored co-chaperone homolog in the  
781 chloroplast protein translocon. *EMBO J* 22:2970–2980 (2003).

782